Parasitology Research (2019) 118:1205–1214
https://doi.org/10.1007/s00436-019-06276-z

HELMINTHOLOGY - ORIGINAL PAPER

First ultrastructural and cytochemical data on the spermatozoon and its differentiation in progenetic and adult *Archigetes sieboldi* Leuckart, 1878 (Cestoda, Caryophyllidea, Caryophyllaeidae)

Magdaléna Bruňanská[1] · Martina Matoušková[1] · Jana Nebesářová[2,3] · John S. Mackiewicz[4] · Larisa G. Poddubnaya[5]

Received: 12 December 2018 / Accepted: 26 February 2019 / Published online: 7 March 2019

Abstract

Spermiogenesis in progenetic and adult stages of *Archigetes sieboldi* Leuckart, 1878, a tapeworm parasitic in oligochaetes and fish respectively, has been examined using transmission electron microscopy and cytochemical staining for glycogen. General pattern of spermiogenesis is essentially like that of other caryophyllideans, i.e., apical dense material in the zone of differentiation in the early stages of spermiogenesis, rotation of free flagellum and a flagellar bud, and proximo-distal fusion. Interestingly, rotation of a free flagellum and flagellar bud to the median cytoplasmic process (MCP) has been observed unconventionally at > 90° only in progenetic stages. Typical striated roots associated with the centrioles occur rarely in *A. sieboldi*, and only in form of faint structures in advanced stages of spermiogenesis. In contrast to most caryophyllideans studied to date, penetration of the nucleus into the spermatid body has started before the fusion of the free flagellum with the MCP. This feature has been reported rarely but exclusively in the family Caryophyllaeidae. The unipartite mature spermatozoon of *A. sieboldi* is composed of one axoneme of the 9 + '1' trepaxonematan pattern with its centriole, parallel nucleus, and parallel cortical microtubules which are situated in a moderately electron-dense cytoplasm with glycogen particles. An unusual arrangement of cortical microtubules in the two parallel rows in region I of the spermatozoon is described here for the first time in the Caryophyllidea. Ultrastructural data on spermiogenesis and the spermatozoon in *A. sieboldi* from tubuficids and carp are compared and discussed with those in other caryophyllideans and/or Neodermata.

Keywords Caryophyllidea · *Archigetes sieboldi* · Spermiogenesis · Spermatozoon · Ultrastructure

Section Editor: David Bruce Conn

✉ Magdaléna Bruňanská
brunan@saske.sk

[1] Institute of Parasitology, Slovak Academy of Sciences, Hlinkova 3, 040 01 Košice, Slovak Republic

[2] Institute of Parasitology, Biology Centre of the Czech Academy of Sciences, České Budějovice, Czech Republic

[3] Faculty of Science, University of South Bohemia, České Budějovice, Czech Republic

[4] Department of Biological Sciences, University at Albany, State University of New York, Albany, NY, USA

[5] I. D. Papanin Institute for Biology of Inland Waters, Russian Academy of Sciences, Borok, Yaroslavl Province, Russia

Introduction

Archigetes sieboldi Leuckart, 1878 is monozoic tapeworm characterized by two basic modes of life cycle: (1) two-host life cycle which is most common for the Caryophyllidea and (2) a monoxenic one occurring in specimens from a tubificid annelid. *Archigetes* has a long history (see Mackiewicz 1981, 2003; Poddubnaya 2003; Poddubnaya et al. 2003; Olson et al. 2008). However, questions regarding the evolutionary significance of this enigmatic tapeworm and phylogenetic relationships within the Caryophyllidea are still not resolved (Waeschenbach et al. 2012; Caira and Littlewood 2013).

Spermatology characters might be useful for phylogenetic analysis of various organisms, including the Eucestoda (Justine 1998, 2001, 2003; Hoberg et al. 2001; Bruňanská 2010; Levron et al. 2010). Within the

Caryophyllidea, spermatological data are available for 12 species from three families (out of four currently recognized: Balanotaeniidae, Capingentidae, Caryophyllaeidae, Lytocestidae). *A. sieboldi* belongs to the family Caryophyllaeidae which comprises 20 genera and about 80 nominal species. Ultrastructural studies on spermato/spermiogenesis and/or the spermatozoon within the Caryophyllaeidae have been done on four species only: *Glaridacris catostomi* Cooper, 1920, *Wenyonia virilis* Woodland, 1923, *Caryophyllaeus laticeps* (Pallas, 1781), and *Hunturella nodulosa* Mackiewicz and McCrae, 1962 (see Kazacos and Mackiewicz 1972; Świderski and Mackiewicz 2002; Gamil 2008; Miquel et al. 2008; Bruňanská and Kostič 2012; Yoneva et al. 2012a).

The present study aims to elucidate the cytodifferentiation and fine structural organization of male gametes in *A. sieboldi*, another evolutionarily attractive cestode of the family Caryophyllaeidae. The two developmental stages, progenetic caudate plerocercoids and adult specimens are the subject of this investigation. Our results will provide additional phylogenetically important data which may contribute to a better understanding of reproductive biology in the Caryophyllidea.

Materials and methods

Two developmental stages of *Archigetes sieboldi* were investigated: (1) progenetic caudate plerocercoids (terminology of Chervy 2002) or procercoid or progenetic procercoid of previous authors (see Poddubnaya et al. 2003 for views on terminology) recovered from the coelom of the tubificid oligochaete, *Limnodrilus hoffmeisteri* Claparède, collected in the Latka River (Yaroslavl Province, Russia), and (2) adult specimens from the intestine of *Cyprinus carpio* caught in the Tisa River, Slovakia. Live specimens were fixed using 3% glutaraldehyde in 0.1 M cacodylate buffer (pH 7.4) for 10 h at 4 °C, postfixed in 2% OsO_4 in 0.1 M cacodylate buffer for 2 h at 4 °C, dehydrated in a graded series of ethanol, and embedded in Spurr epoxy resin. Semithin sections were cut with glass knives on an ultramicrotom LKB Bromma 8880, stained with methylene blue, and examined under a light microscope for localization of testes and vas deferens. Ultrathin sections were cut with a diamond knife on a Leica Ultracut UCT ultramicrotome, placed on copper grids and double stained with uranyl acetate and lead citrate. The grids were examined in a JEOL 1010 transmission electron microscope operating at 80 kV.

The periodic acid-thiosemicarbazide-silver proteinate (PA-TSC-SP) technique of Thiéry (1967) was applied for detection-specific cytochemical localization of glycogen.

Results

Spermiogenesis

The beginning of spermiogenesis of *Archigetes sieboldi* is characterized by formation of the zone of differentiation (ZD) at the periphery of each spermatid (Fig. 1a). It is lined by a submembraneous row of cortical microtubules (CM) and contains a binary complex of the two centrioles with an intercentriolar body (ICB) between them. This binary complex is tightly associated with apical electron-dense material in the early spermatid (Figs. 1b, d, e and 2a, b). One of the centrioles gives rise to a short free flagellum (Fig. 1b) which grows and might be slightly bent towards the base of the spermatid, thus forming an angle of more than 90° to the hypothetical long axis of the spermatid in progenetic caudate plerocercoids (Fig. 1c). A free flagellum and flagellar bud generally grows out in opposite directions from one another (Figs. 1d and 2b) in early stages of spermiogenesis.

The ICB is composed of three electron-dense plates and four electron-lucent zones between them (Figs. 1a–e and 2a–d). Detailed observations reveal two additional thin lines consisting of tiny electron-dense granules situated in the middle of the electron lucent zones (Figs. 1d, inset, and 2a). The two narrow zones of moderate electron density are adjacent to the central electron-dense plate of the ICB.

Fig. 1 Early and advanced stages of spermiogenesis in *Archigetes sieboldi* from oligochaete (**a**, **c**, **h**) and carp (**b**, **d**, **e**, **f**, **g**, **i**, **j**). **a** Early stage of spermiogenesis in longitudinal section of young spermatid includes the two centrioles (C) arranged in the same plane and interconnected with an intercentriolar body (ICB). CM cortical microtubules, N nucleus. Bar = 200 nm. **b** Centriole (C) giving rise to a flagellum (F). ICB intercentriolar body, N nucleus. Bar = 500 nm. **c** The flagellum (F) is slightly bent towards the base of the spermatid in progenetic caudate plerocercoid. C centriole, ICB intercentriolar body. Bar = 200 nm. **d** While flagellum (F) is growing out, flagellar bud (FB) is formed by the second centriole (C) in the early stages of spermiogenesis. ICB intercentriolar body, N nucleus. Bar = 250 nm. Inset: detail of the ICB shows three electron-dense layers (vertical arrows) and two electron lucent zones (1, 2). Note: (i) two subzones of medium electron density (white asterisk) adjacent to the central electron-dense layer and (ii) electron-dense granules (horizontal arrows) scattered in 1 and 2 and creating two additional lines. Bar = 65 nm. **e** Flagellum (F) and flagellar bud (FB) start to rotate. CM cortical microtubules, DM dense material, ICB intercentriolar body. Bar = 330 nm. **f** Rotation of a flagellum (F) and flagellar bud (FB) in advanced stages of spermiogenesis. AM arching membranes, C centriole, MCP median cytoplasmic process, R striated root. Bar = 500 nm. **g** Cross section illustrates that the nucleus (N) penetrates into the median cytoplasmic process (MCP) before proximodistal fusion of the flagellum with MCP. CM cortical microtubules. Bar = 250 nm. **h** Longitudinal section of the spermatid in advanced stages of spermiogenesis shows that both centrioles (C) with the flagellum (F) and flagellar bud (cutoff) rotate towards the MCP. AM arching membranes, R striated root Bar = 200 nm. **i** Cross section of spermatids before and after proximodistal fusion. Ax axoneme, F flagellum, MCP median cytoplasmic process. Bar = 250 nm. **j** Longitudinal section of the MCP with incorporated axoneme (Ax) during penetration of the nucleus (N). Bar = 400 nm

The prolongation of both free flagellum and flagellar bud is accompanied by their rotation at 90° (Fig. 1e) in advanced stages of spermiogenesis (Figs. 1f, h and 2c, d). Flagellar rotation proceeds towards the extended median cytoplasmic process (MCP). Even at these stages, it is possible to detect signs of striated roots associated with the centrioles (Figs. 1f, h and 2c, d). A ring of arching membranes (AMs) line the ZD in the proximal extremity and consists of a double membrane situated under the cell membrane of the spermatid.

Transverse sections indicate that migration of the nucleus into the MCP takes place before the fusion of the free flagellum with the MCP (Fig. 1g). Flagellar rotation of the free flagellum (having typical trepaxonematan 9 + '1' structure) and flagellar bud is followed by proximodistal fusion of the free flagellum with the MCP (Figs. 1h–j and 2d, e). At the end

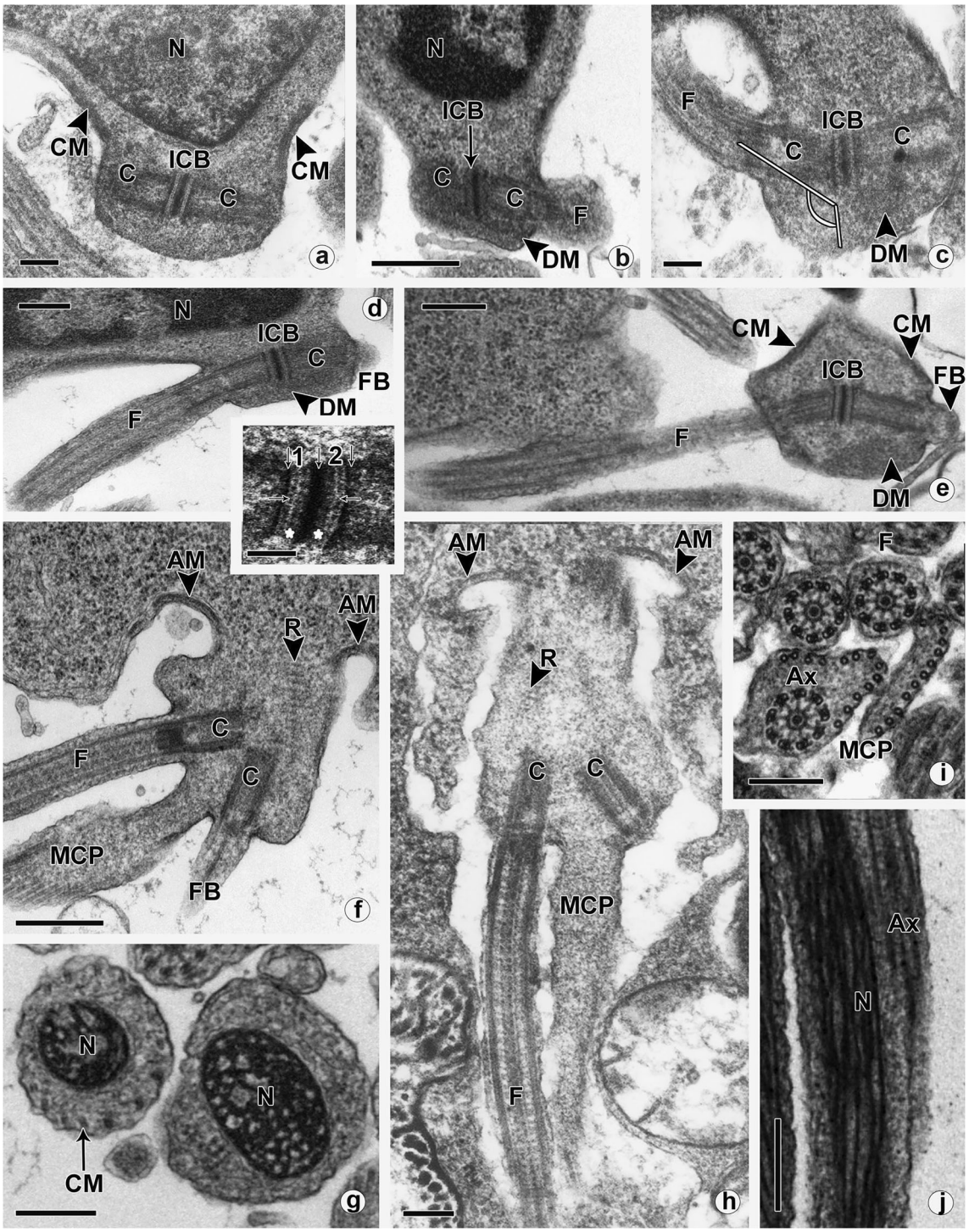

of spermiogenesis, the constriction of the ring of the AM enables final liberation of the spermatozoon from residual cytoplasm.

Mature spermatozoon

The filiform mature spermatozoon of *A. sieboldi* contains one axoneme of the 9 + '1' trepaxonematan type, parallel cortical microtubules, glycogen granules, and a nucleus that is parallel to the axoneme. The middle part of the sperm body includes electron-dense attachment zones. The male gamete can be divided into five regions of distinctive ultrastructural organization (I–V).

Region I (Figs. 3a–e and 4I) conforms to the proximal (or anterior) extremity of the spermatozoon. At first, the central complex core unit of the centriole is tightly surrounded by nine singlet tubular structures which undergo transformation into doublets, now being interconnected to the central complex core unit via short thin electron-dense arms (Fig. 3a, b). One set of a few (up to 5) cortical microtubules (CM) is arranged in a semiarc beneath the plasma membrane. The diameter of the cell is approximately 130 nm at this centriolar region (Fig. 3a) and gradually increases up to approximately 270 nm with the following appearance of the complete axoneme (Fig. 3c). Mostly, up to six CM occur in this region. Occasionally, the CM are arranged into two parallel rows: the inner one consisting of five tubules and the peripheral row including six tubules (Fig. 3d). These two rows are consequently unified into one semicircle made up of 12 tubules (Fig. 3e).

Region II (Figs. 3f, g and 4II) is a short transition zone characterized by a bipolar shape of the sperm body in cross section, showing one axoneme on one side, and the cytoplasm filled with scattered electron-dense granules, and possessing a continuous row of CM (up to 10) under the plasma membrane, on the opposite side (Figs. 3f and 4II). Cytoplasmic electron-dense granules are identified as glycogen using the Thiéry method (Fig. 3g). One pair of attachment zones (indicating the points of fusion of the free flagellum with the MCP) can be detected in cross sections (Fig. 3f, g). The transverse sections of the region II of the spermatozoon measure about 520 nm in diameter (Fig. 3g).

Region III (Figs. 3h–k and 4III) constitutes a middle portion of the sperm body that is bipolar shaped in cross sections with one axoneme on one side and on the opposite side an electron-dense nucleus in an enlarged cytoplasmic area. The nucleus is roughly circular-shaped, with diameter measuring around 30 nm at the anterior part (Fig. 3h), 270 nm in the middle part (Fig. 3j), and 200 nm in the more posterior part of region III (Fig. 3k). A pair of attachment zones are present in the anterior half of region III (Figs. 3h–j). The CM are scattered under the plasma membrane in the nuclear area, and some of them come into close contact with it. The number of CM is reduced gradually with its maximum (up to 9) at the beginning and minimum (2) at the end of the region III, where the nucleus disappears. The spermatozoon width in the region III is about 535 nm.

Region IV (Figs. 3l and 4IV) exhibits still reduced diameter of the spermatozoon (approximately 495 nm) due to reduction of the cytoplasm volume. One axoneme and only a few cortical microtubules are present (Fig. 3l).

Region V (Figs. 3m, n and 4V) conforms to the posterior extremity of the spermatozoon. CM disappear (Fig. 3m) and the axoneme becomes disorganized. The central core structure disappears first, and the number of doublets is gradually reduced. The very posterior extremity of the *A. sieboldi* spermatozoon is around 155 nm in diameter, and contains doublets and singlets of the disorganized axoneme (Fig. 3n).

Discussion

Our detailed ultrastructural and cytochemistry analysis gives evidence that the male reproductive system is fully functional in progenetic caudate plerocercoids of *Archigetes sieboldi* as suggested earlier (Poddubnaya et al. 2003). While the reproductive system is fully functional, i.e., capable of producing another cestode, it does so in the invertebrate cycle by rupturing the gravid stage within the killed oligochaete and disseminating the eggs in the aquatic environment. Because the gonopores are not functional in the progenetic stage, this mode of egg dissemination in the *A. sieboldi* cycle kills both the cestode and the host oligochaete. A similar cycle has been described for *Archigetes iowensis* by Calentine (1964). The oligochaete becomes infected by ingesting mud containing the infective eggs. As far as is known, fish only become infected by consuming oligochaetes with infective larval cestode stages. The only difference between spermiogenesis in the two developmental stages from different hosts concerns the free flagellum forming an angle > 90° to the long axis of early spermatid in *A. sieboldi* progenetic caudate plerocercoids from oligochaetes, but not in the mature worms from fish.

Our analysis also indicates that a revised model of the caryophyllidean type of spermiogensis by Bruňanská and Kostič (2012) is valid. In contrast to traditional models of spermiogenesis (Świderski 1986; Bâ and Marchand 1995), the present results show that the process of sperm formation in the Caryophyllidea is accompanied by the presence of (1) dense material in early stages of spermiogenesis and (2) the second centriole which gives rise to a flagellar bud rotating synchronously or slightly asynchronously with the free flagellum. These findings were reported during spermiogenesis in some other caryophyllidean cestodes (Bruňanská and Poddubnaya 2006; Bruňanská 2009, 2010; Miquel et al. 2008; Yoneva et al. 2011, 2012a, b; Matoušková et al. 2018) and support a derived stage of spermiogenesis, as a rotating flagellar bud clearly represents an evolved character in the Caryophyllidea.

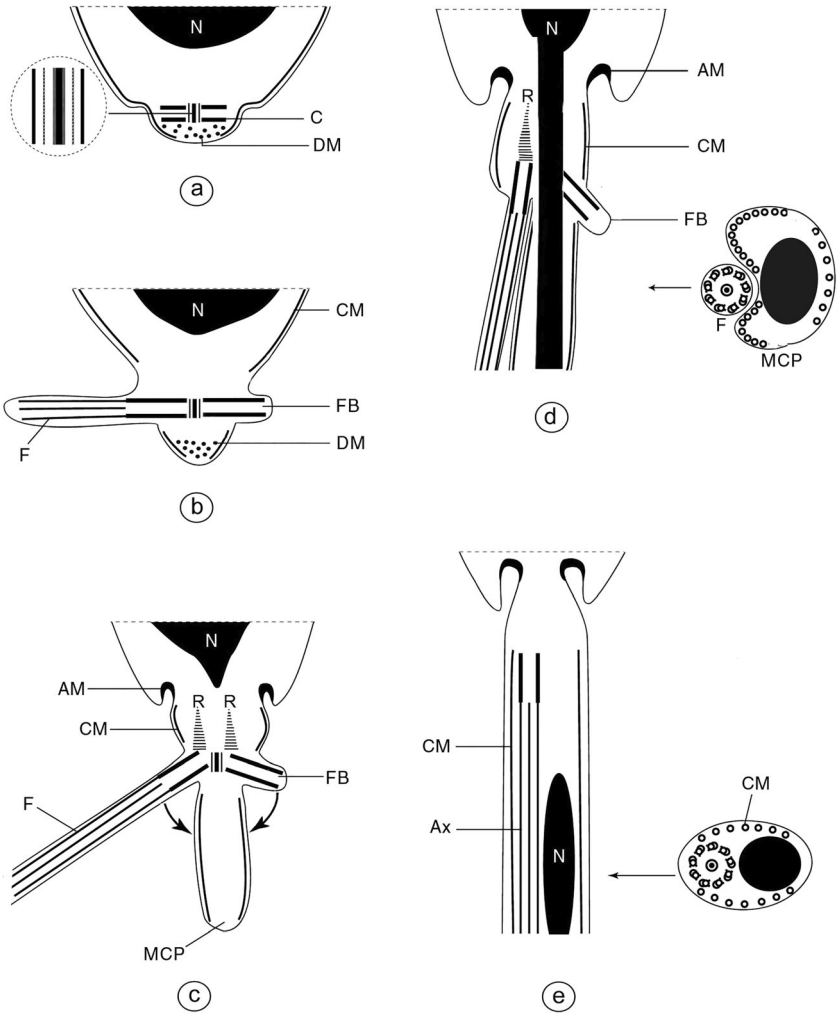

Fig. 2 Schematic reconstruction of the main consecutive stages of spermiogenesis in *A. sieboldi* (**a**, **b** early stages; **c**, **d** advanced stages; **e** final stage of spermiogenesis). AM arching membrane, Ax axoneme, C centriole, CM cortical microtubules, DM apical electron-dense material, F flagellum, FB flagellar bud, ICB intercentriolar body, MCP median cytoplasmic process, N nucleus, R striated root

Apical dense material is associated with initial stages of spermiogenesis in those non-cyclophyllidean cestodes which exhibit either one-axoneme spermatozoon, e.g., caryophyllideans (Bruňanská and Poddubnaya 2006; Gamil 2008; Miquel et al. 2008; Bruňanská 2009, 2010; Yoneva et al. 2011, 2012a, b; Bruňanská and Kostič 2012; Matoušková et al. 2018; present study), or two-axoneme spermatozoon, e.g., amphilinideans (Bruňanská et al. 2013), spathebothriideans (Bruňanská et al. 2006; Bruňanská and Poddubnaya 2010), bothriocephalideans (Bruňanská et al. 2001; Levron et al. 2005, 2006a; Šípková et al. 2010, 2011; Marigo et al. 2012a), diphyllobothriideans (Levron et al. 2006b, 2009, 2013; Yoneva et al. 2013), and some proteocephalideans (Marigo et al. 2012b). It was clearly shown that the apical dense material is usually very closely associated with the appearance, and thus with origin of three basic structures: (1) a centriole, (2) striated root, and (3) an intercentriolar body in initial stages of spermiogenesis in cestodes exhibiting this cell element (see e.g. Bruňanská et al. 2001). However, further studies are necessary to elucidate in more detail the function of apical dense material.

Each centriole is associated with a typical striated root during spermiogenesis of Types I and II in the Eucestoda (Bâ and Marchand 1995). However, typical striated roots were never detected in early stages of spermiogenesis in the present study; they appear as a very faint structures in advanced stages of the process. We suppose that this unusual feature may be related to the two basic modes of life cycle in *A. sieboldi*, i.e., in oligochaete or fish host. Interestingly, the absence of typical striated rootlets in non-cyclophyllideans has been reported in *Nippotaenia mogurndae*, a more derived cestode producing a single axoneme spermatozoon during spermiogenesis of the same type as is described in the Caryophyllidea (see Bruňanská et al. 2015). However, in contrast to *A. sieboldi*, nippotaeniid exhibits very thin striated structures associated with each centriole during spermiogenesis.

The intercentriolar body (ICB) appears in the zone of differentiation of early spermatid of *A. sieboldi*. Within the Caryophyllidea, the ICB comprises either a number of parallel disc-shaped plates of different electron density (see Świderski and Mackiewicz 2002), or the number of plates is reduced most often to five plates (three of them are electron-dense)

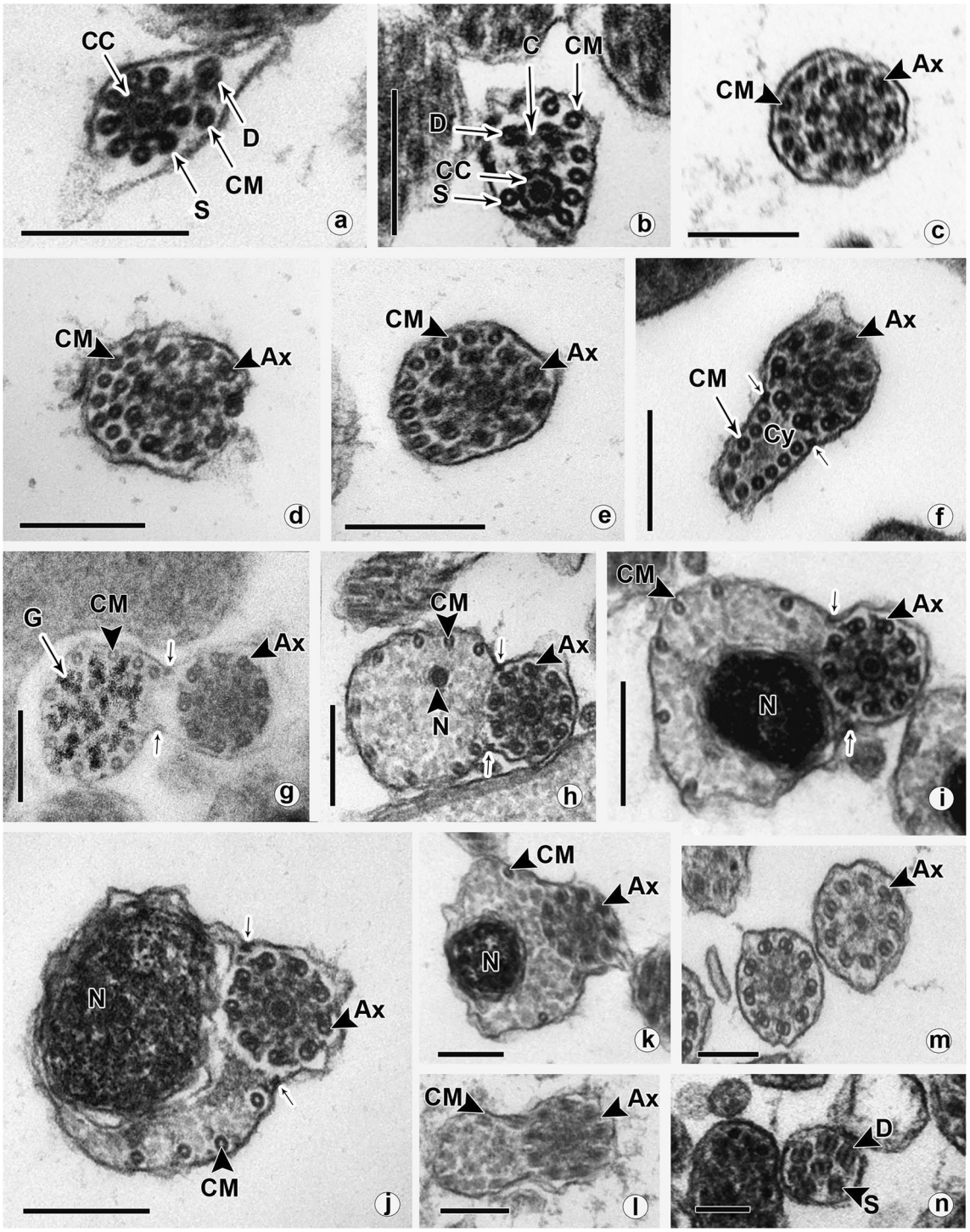

(Miquel et al. 2008; Bruňanská 2009, 2010; Yoneva et al. 2011, 2012a, b; Bruňanská and Kostič 2012; Matoušková et al. 2018; present study). With the latter array of characters, the ICB in caryophyllideans resembles that structure in amphilinideans (Bruňanská et al. 2013), spathebothriideans (Bruňanská et al. 2006; Bruňanská and Poddubnaya 2010), or bothriocephalideans (Bruňanská et al. 2001; Levron et al. 2005, 2006a, c). Alternatively, the ICB in caryophyllideans was reported to be comprised of a single electron-dense plate (Bruňanská and Poddubnaya 2006), However, in contrast to other caryophyllideans, the ICB of *A. sieboldi* includes two unique features concerning (i) the presence of the two additional very thin electron-dense plates and (ii) the central electron-dense plate which is bordered with two plates of lower electron density (compare Fig. 1d, inset in the present study). The presence of the two additional very thin

◀ **Fig. 3** Ultrastructure of the mature spermatozoa of *A. sieboldi* from carp. **a** Cross section of the anterior extremity of the region I reveals the centriole which is made up of eight singlets (S) that radiate outward from the central complex core unit (CC). Note peripheral doublet (D) and a single cortical microtubule (CM). Bar = 200 nm. **b** Subsequent serial cross section shows that singlets (S) surrounding the central complex core unit (CC) of the centriole (C) are progressively replaced by doublets (D). Note increasing number of cortical microtubules (CM). Bar = 200 nm. **c** Cross section of the region I with a fully formed axoneme (Ax) and semiarc of cortical microtubules (CM). Bar = 250 nm. **d** Cortical microtubules (CM) might be arranged in two parallel rows: peripheral row consisting of six microtubules and the inner row containing five microtubules. Ax axoneme. Bar = 200 nm. **e** The number of cortical microtubules (CM) is increased up to 12. Bar = 200 nm. **f** Cross section of the beginning of the region II with an increasing volume of cytoplasm (Cy) and the attachment zones (small arrows). Ax axoneme, CM cortical microtubules. Bar = 200 nm. **g** Visualization of glycogen (G) using Thiéry method in cross section section of the spermatozoon (region II). Ax axoneme, CM cortical microtubules. Small arrows indicate attachment zones. Bar = 200 nm. **h** Cross section of region III with the proximal part of the nucleus (N). Ax axoneme, CM cortical microtubules. Bar = 200 nm. **i** An enlarged profile of nucleus (N) in cross section of region III. The number of cortical microtubules (CM) is increased. Ax axoneme. Small arrows indicate attachment zones. Bar = 250 nm. **j** The central part of region III with large profile of the nucleus (N) and a few cortical microtubules (CM). Ax axoneme. Bar = 200 nm. **k** Cross section of region IV with smaller profile of nucleus (N) and two cortical microtubules (CM). Ax axoneme. Bar = 165 nm. **l** Cross section of region IV. Ax axoneme, CM cortical microtubules. Bar = 165 nm. **m** Cross section of region V. Ax axoneme. Bar = 165 nm. **n** Doublets (D) and singlets (S) of the disorganized axoneme in cross section of posterior extremity of region V. Bar = 100 nm

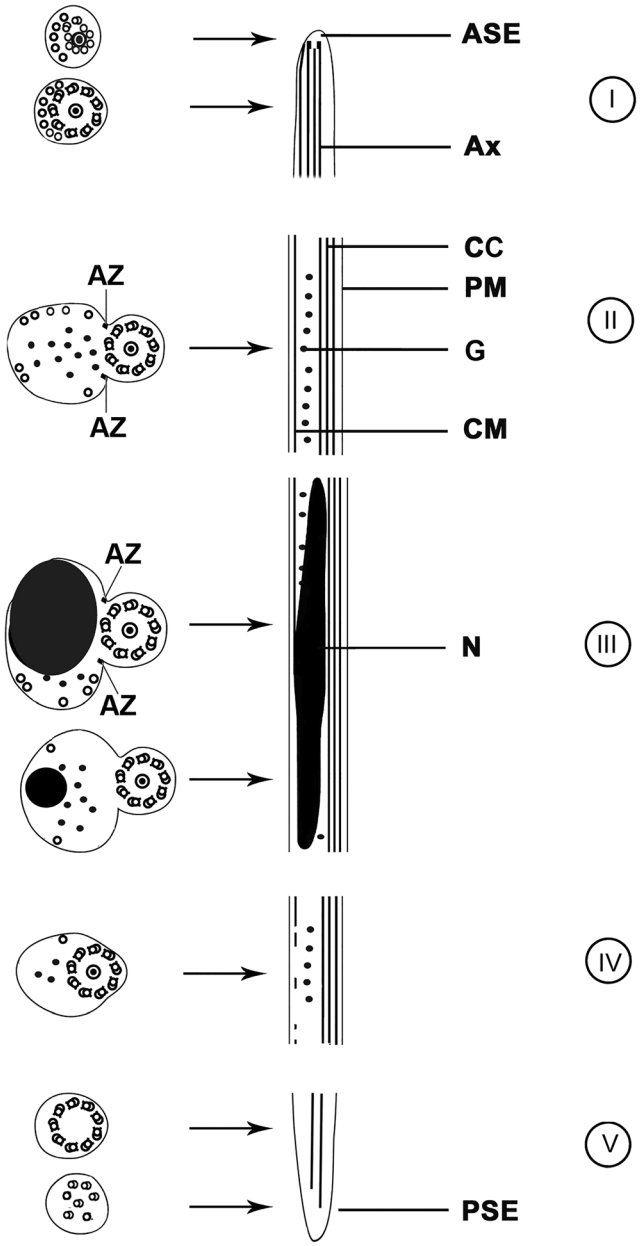

Fig. 4 Schematic reconstruction of the five regions of mature spermatozoon of *A. sieboldi* from carp. ASE anterior spermatozoon extremity, Ax axoneme, AZ attachment zones, CC complex central core unit, CM cortical microtubules, G glycogen, N nucleus, PM plasma membrane, PSE posterior spermatozoon extremity

electron-dense plates may indicate the relationship of *Archigetes* to the cestodes with the ICB composed of five distinct electron-dense plates, i.e., diphyllobothriideans (Levron et al. 2009, 2013; Yoneva et al. 2013). Hereby, it may represent another support of a presumed sister relationship of Caryophyllidea and Diphyllobothriidea (Olson et al. 2008).

A remarkable feature concerns the free flagellum forming an angle > 90° to the long axis of early spermatid in *A. sieboldi* progenetic caudate plerocercoids but not in mature worms. Similar feature was described in the two cestodes only, namely caryophyllidean *Wenyonia* by Miquel et al. (2008), spathebothriidean *Cyathocephalus truncatus* by Bruňanská et al. (2006), and some digeneans (see Levron et al. 2003, 2004; Ndiaye et al. 2003a; Agostini et al. 2005). This fact is interesting when considering specific two basic modes of life cycle in *A. sieboldi*, unusual morphological characteristics of *Wenyonia*, and finally, the basal position of the Caryophyllidea and Spathebothriidea within the Eucestoda.

Two different timings of penetration of the nucleus into the spermatid body have been reported in advanced stages of spermiogenesis in the Eucestoda. Usually, the nucleus enters into the spermatid body after proximodistal fusion of the free flagellum with the median cytoplasmic process (MCP) (Bruňanská 2010). In contrast, migration of the nucleus into the MCP has been observed before the proximodistal fusion in some caryophyllideans exclusively of the family Caryophyllaeidae (Gamil 2008; Miquel et al. 2008; Yoneva et al. 2012a; present study), tetraphyllideans (Mokhtar-Maamouri and Świderski 1975), and proteocephalideans (Świderski 1985), and cyclophyllideans (Miquel et al. 1999). These findings fail to support hypothesis that migration of the nucleus is induced by lateral fusion of free flagellum with the MCP (Świderski 1985).

Although the ultrastructural organization of the mature spermatozoon of *A. sieboldi* principally resembles that of other Caryophyllidea in having one axoneme, parallel cortical microtubules, and nucleus (Bruňanská 2010; Levron et al. 2010), some different particularities have been observed in the present study. For the first time in the Caryophyllaeidae, the centriolar part and an unusual arrangement of cortical microtubules are described in region I of the mature spermatozoon. A notable feature of the mature male gamete is the occurrence of the two attachment zones in its principal regions.

The centriole has been described rarely in the mature spermatozoa of the Eucestoda. In contrast to *A. sieboldi* exhibiting nine singlet tubular structures surrounding a central complex core unit at the most proximal proximity of the centriole, in another caryophyllidean, lytocestid *Khawia sinensis*, nine doublets were detected around the central structure of the centriole (Bruňanská 2009). Interestingly, both singlets and doublets have been described in the centriole of the mature spermatozoon of spathebothriidean *Didymobothrium rudolphii* (Bruňanská and Poddubnaya 2010), diphyllobothriidean *Cephalochlamys namaquensis* by Bruňanská et al. (2012a), and in the proteocephalidean *Electrotaenia malopteruri* by Bruňanská et al. (2004a). However, the centriole is surrounded by a few cortical microtubules (1–3) in the above caryophyllideans, spathebothriidean, and diphyllobotriidean, whereas a semicircle of up to 14 cortical microtubules is present in the proteocephalid cestode, in some tetraphyllideans (Marigo et al. 2011a), trypanorhynchs (Miquel and Świderski 2006; Miquel et al. 2007; Marigo et al. 2011b), and bothriocephalideans (Levron et al. 2006c; Marigo et al. 2012a). These findings may give further evidence of the close relationship of the Caryophyllidea, Spathebothriidea, and Diphyllobothriidea, and support the fact that the centriole is a base of the axoneme in the Eucestoda with the 9 + '1' pattern of the Trepaxonemata.

An unusual arrangement of cortical microtubules in two parallel rows in region I of the mature spermatozoon of *A. sieboldi* is described for the first time in the Caryophyllidea. It was reported in anucleated region II of the spermatozoon of spathebothriidean *D. rudolphii* by Bruňanská and Poddubnaya (2010), and in late spermatids (not in the mature spermatozoon) of proteocephalidean *Corallobothrium solidum* (see Bruňanská et al. 2004b, 2005). Occurrence of this rare feature in the mature spermatozoa of *Archigetes* may be related to the basal position of the Caryophyllidea and Spathebothriidea.

One pair of attachment zones (AZ) in the principal region of the spermatozoon of *A. sieboldi* corresponds to the points of fusion of the free flagellum with the MCP during spermiogenesis. This pattern was reported in one-axoneme spermatozoa of two lytocestid caryophylideans, *Lytocestus indicus* and *Caryophyllaeides fennica* (Yoneva et al. 2012b; Matoušková et al. 2018), and cyclophyllideans (e.g., Ndiaye et al. 2003b). On the other hand, the AZ were detected in the two-axoneme spermatozoa of amphilinideans (Bruňanská et al. 2012b), spathebothriideans (Bruňanská et al. 2006; Bruňanská and Poddubnaya 2010), bothriocephalideans (Levron et al. 2006a, c; Marigo et al. 2012a), diphyllobothriideans (Levron et al. 2006b, 2009, 2013; Bruňanská et al. 2012a), and trypanorhynchs (Miquel and Świderski 2006; Miquel et al. 2007; Marigo et al. 2011b).

Ultrastructural data on the spermatozoon and its differentiation in *A. sieboldi* favor hypothesis that the monozoic condition of the Caryophyllidea is secondarily derived from an ancestor closely allied with a polypleuroid or strobilate tapeworms with a 2-axoneme spermatozoon (Fuhrman 1931; Joyeux and Baer 1961; Mackiewicz 1981, 2003). However, definitive elucidation of phylogenetic relationships among lower cestodes needs further complex studies integrating ultrastructural, morphological, and molecular data.

Acknowledgements We would like to thank our colleague Mikuláš Oros (Slovakia) for providing invaluable help with collecting parasites. This study was supported by the Grant Agency of the Slovak Republic VEGA (project no. 2/0104/16 to MB). We acknowledge the core facility of the Institute of Parasitology, BC ASCR in České Budějovice, Czech Republic, supported by the MEYS CR (LM2015062 Czech-BioImaging). This research was undertaken within the framework of a joint research project nos. AV ČR-16-08 and SAV-18-21 supported by a bilateral agreement on scientific exchange and cooperation signed by the Czech and Slovak Academies of Sciences.

Compliance with ethical standards

Conflict of interest The authors declare that they have no conflict of interest.

References

Agostini S, Miquel J, Ndiaye PI, Marchand B (2005) *Dicrocoelium hospes* Looss, 1907 (Digenea, Dicrocoeliidae): spermiogenesis, mature spermatozoon and ultrastructural comparative study. Parasitol Res 96:38–48

Bâ CT, Marchand B (1995) Spermiogenesis, spermatozoa and phyletic affinities in the Cestoda. In: Jamieson, BGM, Ausie J, Justine J-L (eds) advances in Spermatozoal phylogeny and taxonomy. Mém Mus natn Hist nat 166:87–95

Bruňanská M (2009) Spermatological characters of the caryophyllidean cestode *Khawia sinensis* Hsü, 1935, a carp parasite. Parasitol Res 105:1603–1610

Bruňanská M (2010) Recent insights into spermatozoa development and ultrastructure in the Eucestoda. In: Lejeune T, Delvaux P (eds) Human spermatozoa: maturation, capacitation and abnormalities. Nova Science Publishers, Inc., New York, pp 327–354

Bruňanská M, Kostič B (2012) Revisiting caryophyllidean type of spermiogenesis in the Eucestoda based on spermatozoon differentiation and ultrastructure of *Caryophyllaeus laticeps* (Pallas, 1781). Parasitol Res 110:141–149

Bruňanská M, Poddubnaya LG (2006) Spermiogenesis in the caryophyllidean cestode *Khawia armeniaca* (Cholodkovski, 1915). Parasitol Res 99:449–454

Bruňanská M, Poddubnaya LG (2010) Spermatological characters of the spathebothriidean tapeworm *Didymobothrium rudolphii* (Monticelli, 1890). Parasitol Res 106:1435–1442

Bruňanská M, Nebesářová J, Scholz T, Fagerholm H-P (2001) Spermiogenesis in the pseudophyllid cestode *Eubothrium crassum* (Bloch, 1779). Parasitol Res 87:579–588

Bruňanská M, Scholz T, Ibraheem MH (2004a) Ultrastructural particularities of the spermatozoon of the cestode *Electrotaenia malopteruri* (Fritsch, 1886) (Proteocephalidae: Gangesiinae), a parasite of *Malapterurus electricus* (Siluriformes: Malapteruridae) from the Nile, Egypt. Parasitol Res 93:114–120

Bruňanská M, Scholz T, Ibraheem MH (2004b) Ultrastructural characteristics of the spermatozoon of the cestode *Corallobothrium solidum* Fritsch, 1886 (Proteocephalidae: Corallobothriinae), a parasite of *Malapterurus electricus* (Siluriformes: Malapteruridae) from the Nile, Egypt. Parasitol Res 94:421–426

Bruňanská M, Scholz T, Ibraheem MH (2005) Spermiogenesis in the cestode *Corallobothrium solidum* Fritsch, 1886 (Proteocephalidae: Corallobothriinae), parasite of *Malapterurus electricus* (Siluriformes: Malapteruridae) from the Nile, Egypt. Acta Zool 86: 55–61

Bruňanská M, Scholz T, Dezfuli B, Poddubnaya LG (2006) Spermiogenesis and sperm ultrastructure of *Cyathocephalus truncatus* (Pallas, 1781) Kessler, 1868 (Cestoda: Spathebothriidea). J Parasitol 92:884–892

Bruňanská M, Matey V, Nebesářová J (2012a) Ultrastructure of the spermatozoon of the diphyllobothriidean cestode *Cephalochlamys namaquensis* (Cohn, 1906). Parasitol Res 111:1037–1043

Bruňanská M, Poddubnaya LG, Xylander WER (2012b) Spermatozoon cytoarchitecture of *Amphilina foliacea* (Platyhelminthes, Amphilinidea). Parasitol Res 111:2063–2069

Bruňanská M, Poddubnaya LG, Xylander WER (2013) A reinvestigation of spermiogenesis in *Amphilina foliacea* (Platyhelminthes, Amphilinidea). Folia Parasitol 60:43–50

Bruňanská M, Bílý T, Nebesářová J (2015) *Nippotaenia mogurndae* Yamaguti et Myiata, 1940 (Cestoda, Nippotaeniidea): first data on spermiogenesis and sperm ultrastructure. Parasitol Res 114:1443–1453

Caira JN, Littlewood DTJ (2013) Worms, Platyhelminthes. In: Levin SA (ed) Encyclopedia of biodiversity, Academic press, vol 7, Waltham, pp 437–469

Calentine R (1964) The life cycle of *Archigetes iowensis* (Cestoda: Caryophyllaeidae). J Parasitol 50:454–458

Chervy L (2002) The terminology of larval cestodes or metacestodes. Syst Parasitol 52:1–33

Fuhrman O (1931) Dritte Klasse des Cladus Plathelminthes: Cestoides. In: Kükenthal W, Krumbach T (eds) Handbuch der Zoologie. Walter de Gruyter and Co., Berlin, pp 141–416

Gamil IS (2008) Ultrastructural studies of the spermatogenesis and spermiogenesis of the caryophyllidean cestode *Wenyonia virilis* (Woodland, 1923). Parasitol Res 103:777–785

Hoberg EP, Mariaux J, Brooks DR (2001) Phylogeny among the orders of the Eucestoda (Cercomeromorphae): integrating morphology, molecules and total evidence. In: Littlewood DTJ, Bray RA (eds) Interrelationships of the Platyhelminthes. Taylor and Francis, London, pp 112–126

Joyeux CH, Baer JG (1961) Classe des Cestodes. In: Grassé P-P (ed) Traité de Zoologie, Tome 4, Fasc, vol 1. Masson, Paris, pp 345–560

Justine J-L (1998) Spermatozoa as phylogenetic characters for the Eucestoda. J Parasitol 84:385–408

Justine J-L (2001) Spermatozoa as phylogenetic characters for the Platyhelminthes. In: Littlewood DTJ, Bray RA (eds) Interrelationships of the Platyhelminthes. Taylor and Francis, London, pp 231–238

Justine J-L (2003) Ultrastructure des spermatozoïdes et phylogénie des Neodermata. In: C. Combes C, Jourdane J (eds) Taxonomy, ecology and evolution of metazoan parasites. PUP, Perpignan, pp 359–380

Kazacos K, Mackiewicz JS (1972) Spermatogenesis in *Hunturella nodulosa* Mackiewicz and McCrae, 1962 (Cestoidea: Caryophyllidea). Z Parasitenkd 38:21–31

Levron C, Ternengo S, Marchand B (2003) Ultrastructure of spermiogenesis and the spermatozoon of *Helicometra fasciata* (Digenea, Opecoelidae), a parasite of *Labrus merula* (Pisces, Teleostei). Acta Parasitol 48:255–264

Levron C, Ternengo S, Marchand B (2004) Ultrastructure of spermiogenesis and the spermatozoon of *Monorchis parvus* Looss, 1902 (Digenea, Monorchiidae), a parasite of *Diplodus annularis* (Pisces, Teleostei). Parasitol Res 93:102–110

Levron C, Bruňanská M, Marchand B (2005) Spermiogenesis and sperm ultrastructure of the pseudophyllidean cestode *Triaenophorus nodulosus* (Pallas, 1781). Parasitol Res 98:26–33

Levron C, Bruňanská M, Poddubnaya LG (2006a) Spermatological characters of the pseudophyllidean cestode *Bothriocephalus scorpii* (Müller, 1776). Parasitol Int 55:113–120

Levron C, Bruňanská M, Poddubnaya LG (2006b) Spermatological characters in *Diphyllobothrium latum* (Cestoda, Pseudophyllidea). J Morphol 267:1110–1119

Levron C, Bruňanská M, Kuchta R, Freeman M, Scholz T (2006c) Spermatozoon ultrastructure of the pseudophyllidean cestode *Paraechinophallus japonicus*, a parasite of deep-sea fish *Psenopsis anomala* (Perciformes, Centrolophidae). Parasitol Res 100:115–121

Levron C, Sitko J, Scholz T (2009) Spermiogenesis and spermatozoon of the tapeworm *Ligula intestinalis* (Diphyllobothriidae): phylogenetic implications. J Parasitol 95:1–9

Levron C, Miquel J, Oros M, Scholz T (2010) Spermatozoa of tapeworms (Platyhelminthes, Eucestoda): advances in ultrastructural and phylogenetic studies. Biol Rev 85:523–543

Levron C, Yoneva A, Kalbe M (2013) Spermatological characters in the diphyllobothriidean *Schistocephalus solidus* (Cestoda). Acta Zool (Stockholm) 94:240–247

Mackiewicz JS (1981) Caryophyllidea (Cestoidea): evolution and classification. Adv Parasitol 19:139–206

Mackiewicz JS (2003) Caryophyllidea (Cestoidea): molecules, morphology and evolution. Acta Parasitol 48:143–154

Marigo AM, Eira C, Bâ CT, Miquel J (2011a) Spermatological characters of *Acanthobothrium crassicolle* Wedl, 1855 (Tetraphyllidea, Onchobothriidae), a parasite of the common stingray *Dasyalis pastinaca*. Acta Parasitol 56:191–201

Marigo AM, Świderski Z, Bâ CT, Miquel J (2011b) Spermiogenesis and ultrastructure of the spermatozoon of the trypanorhynch cestode *Aporhynchus menezesi* (Aporhynchidae), a parasite of the velvet belly, lanternshark *Etmopterus spinax* (Elasmobranchii: Etmopteridae). Folia Parasitol 58:69–78

Marigo AM, Delgado E, Torres J, Bâ CT, Miquel J (2012a) Spermiogenesis and spermatozoon ultrastructure of the bothriocephalidean cestode *Clestobothrium crassiceps* (Rudolphi, 1819), a parasite of the teleost fish *Merluccius merluccius* (Gadiformes: Merlucciidae). Parasitol Res 110:19–30

Marigo AM, Levron C, Bâ CT, Miquel J (2012b) Ultrastructural study of spermiogenesis and the spermatozoon of the proteocephalidean cestode *Barsonella lafoni* de Chambrier et al., 2009, a parasite of the catfish *Clarias gariepinus* (Burchell, 1822) (Siluriformes, Clariidae). Zool Anz 251:17–159

Matoušková M, Bílý T, Bruňanská M, Mackiewicz JS, Nebesářová J (2018) Ultrastructure, cytochemistry and electron tomography analysis of *Caryophyllaeides fennica* (Schneider, 1902) (Cestoda:

Lytocestidae) reveals novel spermatology characteristics in the Eucestoda. Parasitol Res 117:3091–3102

Miquel J, Świderski Z (2006) Ultrastructure of the spermatozoon of *Dollfusiella spinulifera* (Beveridge and Jones, 2000) Beveridge, Neifar and Euzet, 2004 (Trypanorhyncha, Eutetrarhynchidae). Parasitol Res 99:37–44

Miquel J, Feliu C, Marchand B (1999) Ultrastructure of spermiogenesis and the spermatozoon of *Mesocestoides litteratus* (Cestoda, Mesocestoididae). Int J Parasitol 29:499–510

Miquel J, Świderski Z, Neifar L, Eira C (2007) Ultrastructure of the spermatozoon of *Parachristianella trygonis* Dollfus, 1946 (Trypanorhyncha, Eutetrarhynchidae). J Parasitol 93:1296–1302

Miquel J, Świderski Z, Mackiewicz JS, Ibraheem MH (2008) Ultrastructure of spermiogenesis in the caryophyllidean cestode *Wenyonia virilis* Woodland, 1923, with re-assessment of flagellar rotation in *Glaridacris catostomi* Cooper, 1920. Acta Parasitol 53: 19–29

Mokhtar-Maamouri F, Swiderski Z (1975) Étude en microscopie électronique de la spermatogénèse de deux cestodes *Acanthobothrium filicolle benedenii* Loennberg, 1889 et *Onchobothrium uncinatum* (Rud., 1819) (Tetraphyllidea, Onchobothriidae). Z Parasitenkd 47:269–281

Ndiaye PI, Miquel J, Fons R, Marchand B (2003a) Spermiogenesis and sperm ultrastructure of the liver fluke *Fasciola hepatica* L., 1758 (Digenea, Fasciolidae): transmission and scanning electron microscopy, and tubulin immunocytochemistry. Acta Parasitol 48:182–194

Ndiaye PI, Miquel J, Marchand B (2003b) Ultrastructure of spermiogenesis and spermatozoa of *Taenia parva* Baer, 1926 (Cestoda, Cyclophyllidea, Taeniidae), a parasite of the common genet (*Genetta genetta*). Parasitol Res 89:34–43

Olson PD, Poddubnaya LG, Littlewood DTJ, Scholz T (2008) On the position of *Archigetes* and its bearing on the early evolution of the tapeworms. J Parasitol 94:898–904

Poddubnaya LG (2003) Ultrastructure of reproductive organs and ducts in the progenetic species *Archigetes sieboldi* (Cestoda: Caryophyllidea). Zool Zh 82:1038–1050 **(In Russian)**

Poddubnaya LG, Mackiewicz JS, Kuperman BI (2003) Ultrastructure of *Archigetes sieboldi* (Cestoda: Caryophyllidea): relationship between progenesis, development and evolution. Folia Parasitol 50:275–293

Šípková L, Levron C, Freeman M, Scholz T (2010) Spermiogenesis and spermatozoon of the tapeworm *Parabothriocephalus gracilis* (Bothriocephalidea): ultrastructural and cytochemical studies. Acta Parasitol 55:58–65

Šípková L, Levron C, Oros M, Justine J-L (2011) Spermatological characters of bothriocephalideans (Cestoda) inferred from an ultrastructural study on *Oncodiscus sauridae* and *Senga* sp. Parasitol Res 109: 9–18

Świderski Z (1985) Spermiogenesis in the proteocephalid cestode *Proteocephalus longicollis*. In: Timme AH (ed) Proceedings of the Electron Microscopical Society of South Africa, 24th annual conference. University of Natal, Pietermaritzburg, pp 181–182

Świderski Z (1986) Three types of spermiogenesis in cestodes. In: Imura T, Maruse S, Suzuki T (eds) Proc 11th Int Congr Electr Microsc, Kyoto, pp 2959-2960

Świderski Z, Mackiewicz JS (2002) Ultrastructure of spermatogenesis and spermatozoa of the caryophyllidean cestode *Glaridacris catostomi* Cooper, 1920. Acta Parasitol 47:83–104

Thiéry J-P (1967) Mise en évidence des polysaccharides sur coupes fines en microscopie électronique. J Microsc 6:987–1018

Waeschenbach A, Webster BL, Littlewood DTJ (2012) Adding resolution to ordinal level relationships of tapeworms (Platyhelminthes: Cestoda) with large fragments of mtDNA. Mol Phylogen Evol 63: 834–847

Yoneva A, Levron C, Oros M, Orosová M, Scholz T (2011) Ultrastructure of spermiogenesis and mature spermatozoon of *Breviscolex orientalis* (Cestoda: Caryophyllidea). Parasitol Res 108:997–1005

Yoneva A, Levron C, Oros M, Orosová M, Scholz T (2012a) Spermiogenesis and spermatozoon ultrastructure of *Hunterella nodulosa* (Cestoda: Caryophyllidea), a monozoic parasite of suckers (Catostomidae) in North America. Folia Parasitol 59:179–186

Yoneva A, Levron C, Ash A, Scholz T (2012b) Spermatological characters of monozoic tapeworms (Cestoda: Caryophyllidea), including first data on a species from the Indomalayan catfish. J Parasitol 98: 423–430

Yoneva A, Kuchta R, Scholz T (2013) Spermiogenesis and sperm ultrastructure of two species of *Duthiersia*, parasites of monitors, with a review of spermatological characters in the Diphyllobothriidea (Cestoda). Zool Anz 252:486–494